Retrieval of monthly average hourly values of direct and diffuse solar irradiance from measurements of global radiation in Spain

A. Pérez-Burgos[a,b,*], M. Díez-Mediavilla[b] C. Alonso-Tristán[b], M.I. Dieste-Velasco[b]

[a] Dpto Física Aplicada, Facultad de Ciencias, Universidad de Valladolid, Spain

[b] Research Group SWIFT (Solar and Wind Feasibility Technologies), Escuela Politécnica Superior (E.P.S), Universidad de Burgos, Spain

[*]**Corresponding author: Ana Pérez-Burgos** Dpto Física Aplicada, Facultad de Ciencias, Universidad de Valladolid, Spain,

Email: anapb@uva.es.

Phone: +34 983 423749

Abstract

An exhaustive evaluation of the performance of decomposition models to estimate direct and diffuse components from the global horizontal solar irradiance has been carried out in this work. The main objective of the work has been to compare the models performance for two different time basis, hourly and monthly average hourly basis. An extensive database of horizontal solar irradiance from nine locations in Spain was used for the study. The data span through January 1980 to December 2012 of hourly solar irradiance for the nine locations, thus, indicates cumulative year sum of 132 years. This study first investigated the decomposition of the hourly horizontal irradiance into hourly direct and diffuse component using six decomposition models widely referenced in the bibliography. On the hourly decomposition investigation, it was observed that there are no significant differences between the six models for each specific location. Nevertheless, the performance of each of the models was strongly dependent on cloudiness conditions and the solar altitude at the location which is associated to the climatic condition of each site. Further investigations using the six decomposition models were conducted to estimate monthly average hourly values of direct and diffuse components of the solar irradiance with proper assessment of the different models performance at the various locations. Based on the results of the investigations which present no significant differences on the performance of the different models, an extremely

simple algorithm was developed to estimate monthly average hourly values of direct and diffuse solar irradiance which reduces the statistical errors in all locations investigated.

Keywords: Solar resource, direct and diffuse solar irradiance, modeling, monthly average hourly values.

1. Introduction

The search for simple, economic and alternative energy solutions which are environmental friendly in meeting small scale energy demand is an emerging need in developed countries [1]. Solar energy plays a crucial role in providing renewable alternative energy for small scale energy demand. Determining the solar radiation components -global, diffuse and direct- or some combination that are applicable to a solar energy conversion system is the first step in evaluating design criteria and performance of solar systems [2].

A very important factor in the assessment of solar energy resources is the availability of high quality solar global, direct and diffuse irradiance data [3,4]; the use of a specific solar component will depend on the energy application involved [2,5-7], direct and diffuse irradiance are required for weather files used in building energy simulations as well as photovoltaic and solar thermal calculations while systems with concentrating optics rely on direct normal irradiance (DNI) availability. The best database would be the long-term collected data at the site of the proposed solar system although it is a difficult task; in the case of DNI, for example, pyrheliometers, installed on devices that track the sun, have a high investment cost and require an intensive labor of monitoring while instrumentation normally used for collection of global horizontal irradiance (GHI) data can be an order of magnitude less expensive and not as labor intensive [8]. This leads to global solar irradiance is more commonly measured at radiometric stations than its components and thus the need for effective models to estimate these ones; the higher or lower complexity of models, accuracy and easy accessibility to input data has been analyzed in several works [9-11].

In a broad sense, models which are able to break down the data into its component parts are called decomposition or separation models. Due to measurements are limited in many radiometric stations in the world, decomposition models are useful tools to obtain new data. For example, in places were global solar irradiance is measured on a daily basis, decomposition models have been used to obtain hourly values from the daily ones [12]. In places where only global solar irradiance is measured, decomposition models have been used to separate the global one into its components direct and diffuse [10, 13-16]. The global radiation decomposition models to direct and diffuse radiations generally use correlations integrating the diffuse fraction K_d, direct radiation transmittance K_b and clearness index K_T. The present work deals with this type of models.

Due to separation models are empirically derived from site-specific measurements, an extensive calibration and performance analysis in different zones is necessary in order to improve their accuracy. Separation models studies have been reported by several authors in the literature: Bertrand et al. [13] evaluate the performance of decomposition models to estimate direct irradiance in Brussels using measurements of GHI as input. Torres et al. [17] compared decomposition models, analyzing the relationship K_d–K_T. Boland et al. [14] show that the decomposition BRL (Boland–Ridley–Lauret) model is well equipped not only to estimate the diffuse solar irradiance but also to estimate the direct one through the chain global-diffuse-DNI. Bortolini et al.[18] analyze three polynomial functions K_d–K_T of ascending degree to estimate the daily diffuse fraction. Yousif et al. [19] determine coefficients of linear correlations K_d–K_T for two locations far from each other and establish that a correlation between K_T and K_d usually exists for any particular place; when a correlation is established for a specific place, then future or past missing data of either direct or diffuse radiation may be estimated in that site. Gueymard and Ruiz-Arias [10], following a thorough literature search, have found 140 separation models since the pioneering, which is an indication of the importance of this topic and of its vitality since the 1960s. According to them, this type of radiation model is ubiquitous to produce solar resource data used in essentially all solar applications.

The error values reported for separation methods depend on the time step basis of data and on the estimated, diffuse or direct, component. Copper et al. [5] estimate both components for four Australian locations and made a comparative study of four separation models on an hourly basis for a minimum of six years for each location; they conclude that RMSE vary between 40 and 65% for the diffuse irradiance and 19-35% for the direct irradiance for the several model-location combinations. Yang et al. [20] show the performance of five decomposition models to estimate the diffuse irradiance for Singapore over a period of one year and report errors which varies from 31.76% to 34.94% . Perez-Burgos et al. [21] analyze the performance of six decomposition models to estimate direct irradiance in Madrid by considering only very clear sky data for the time period 1980-2004 on an hourly basis; they report error values lower than those for all sky conditions so that the best performance, among the studied models, is obtained for Louche model [22] with RMSE= 7.54%.

So far, most of the works done with decomposition models are on an hourly basis. In this work, the behavior of decomposition models to estimate monthly average hourly (MAH) values is evaluated. MAH values are used to visualize a typical average behavior of solar radiation in a specific site; thus, a typical daylight availability in a specific site is usually reported by a chart showing MAH values of solar illuminance [23]; computer tools as *SkyCalc software* provides a chart of MAH values of daylight illumination for a given skylighting design and a particular climate with the aim to help designers quickly determine the skylight strategy for energy savings [24]. In the literature, it was found that some recent papers deal with the solar resource availability based on MAH values in the case of solar illuminance [25, 26], solar direct irradiance [27] and solar ultraviolet radiation [28].

The objective of the paper is to evaluate quantitatively the reliability of decomposition models to estimate direct and diffuse solar radiation on two time-bases: hourly and monthly average hourly basis. With the aim to obtain a conclusive assessment, a broad solar irradiance data from 9 locations in Spain representing different climatic conditions were employed and decomposed using six widely referenced decomposition models. The study also proposed a mathematical algorithm for the estimation of direct and diffuse solar irradiance MAH values.

2. Climatic conditions and experimental data

The experimental data used in this work, supplied by the Spanish National Meteorological Agency (AEMET), consists of hourly horizontal global, diffuse and direct normal irradiance measurements. Data from 5:00 h to 20:00 h were available for each day, time expressed in True Solar Time (TST). The study presents results for nine locations in Spain representing a variety of climatic conditions; the data set used in this study in the 9 locations makes a cumulative total of about 132 years data.

Series provided by AEMET are high quality; nevertheless, some few spurious data have been removed by applying further quality data control described in Li and Lam [29] resulting in 407017 valid data. Table I shows information about the nine locations, time period and number of used data (N). In this table, the *Köppen Climate Classification* has been used to characterize their climatic conditions. Five different sub-climates have been considered in the analysis: *Cfb (temperate oceanic climate),* for Santander and Oviedo locations; *Csb (warm summer mediterranean climate),* for Leon, Valladolid and Salamanca locations; *Bsk (cold semi-arid climate*), for Lleida location; *Csa (hot summer mediterranean climate),* for Madrid and Caceres locations and *Bsh (hot semi-arid* *climate),* for Murcia location. This classification system, although created almost 100 years ago, continues to be one of the most widely used for climate studies in the world. The classification in distinct types of climate is based on average monthly values for precipitation and air temperature. Santander and Oviedo located in the north coast of Spain have abundant precipitations, 1129 mm/year and 960 mm/year, respectively, while Murcia in the East Coast has the minimum rainfall rate, 297 mm/year. Considering location temperatures, Leon is the coldest location with a monthly average temperature varying from 3.2º to 19.8º at different periods of the year while Murcia is the hottest location with ambient temperature range from 10.6º to 27.6º.

Table I: *Geographical characteristics, (latitude, longitude and altitude over the sea level), climate, time period and number of data used (N) for nine locations in Spain.*

Location	Lat. (º)	Long. (º)	Alt. (m)	Climate*	Time Period	N
Santander	43.49	-3.80	52	Cfb	17/06/1999-31/12/2012	35700
Oviedo	43.35	-5.87	336	Cfb	28/06/1999-31/12/2012	32127
Leon	42.59	-5.65	916	Csb	25/08/2006-31/12/2012	20918
Valladolid	41.64	-4.75	735	Csb	01/08/1999-31/12/2012	39871
Salamanca	40.96	-5.50	790	Csb	01/07/2001-31/12/2012	32857
Lleida	41.63	-0.6	192	BSk	05/10/2006-31/12/2012	18366
Madrid	40.45	-3.72	664	Csa	01/01/1980-31/12/2012	107443
Caceres	39.47	-6.34	394	Csa	12/10/1999-31/12/2012	35204
Murcia	38.00	-1.17	61	BSh	01/05/1988-31/12/2012	84531

**Köppen Climate Classification*

3. Description of models

This work deals with decomposition models which calculate solar direct and diffuse irradiance from known data of global irradiance. In some decomposition models, the diffuse component is first evaluated; then the direct component is obtained by the difference between the global and diffuse solar radiations. These algorithms, usually called diffuse fraction models, estimate the diffuse fraction K_d (diffuse to global irradiance ratio) from the clearness index K_T (global irradiance to the corresponding extraterrestrial value ratio) so that the following chain is applied: *Global Rad - K_T - K_d - Diffuse Rad – Direct Rad*. Alternatively, other decomposition models rather use K_T to evaluate the transmittance of beam radiation, K_b (direct to extraterrestrial irradiance ratio) instead of K_d. Here, the chain for the calculation is: *Global Rad - K_T – K_b - Direct Rad - Diffuse Rad* [10, 14]

K_T, K_d and K_b are calculated by:

$$K_T = {}^{G_h}/_{I_0 sin\alpha} \quad (1)$$

$$K_d = {}^{D_h}/_{G_h} \quad (2)$$

$$K_b = {}^{B_h}/_{I_0 sin\alpha} \quad (3)$$

where G_h , D_h and B_h are the global, diffuse and direct irradiance on a horizontal surface and α is the solar altitude angle. K_T, the fraction of the extraterrestrial irradiance that reaches the earth surface is an indicative of the clearness of the atmosphere, K_d express the diffuse portion of the global irradiance and K_b is the fraction of the extraterrestrial irradiance that reaches straight to the earth. I_0 is the extraterrestrial irradiance calculated by:

$$I_0 = I_{SC} E_0 \quad (4)$$

I_{SC} is the solar constant and E_0, the correction factor for the sun-earth distance calculated from the day angle Γ by [30]:

$$E_0 = 1.00011 + 0.034221\cos(\Gamma) + 0.001280\sin(\Gamma) + 0.000719\cos(2\Gamma) + 0.000077\sin(2\Gamma)$$
(5)

Once obtained one of the components, the other is obviously obtained by subtracting from the global one as:

$$G_h = D_h + B_h \quad (6)$$

It is not the aim of this work to make a full revision of existing models but select some well-known representative algorithms; evaluate their performances at different locations such that general conclusions can be applied to others with the same typology [18].

Six models, widely referenced in literature, have been selected; the algorithms, described below (a-f), have been proposed by Reindl et al. [31] (models Reindl1 and Reindl2), Erbs et al. [32], Maxwell [30], Lopez et al. [33] and Louche et al. [22]. The typology of the models [20] show that

Erbs, Reindl1 and Louche used univariate approaches where K_T is the only input. Reindl2, Maxwell and Lopez employed bivariate approaches which involves two inputs, K_T and α. On the other hand, Erbs, Reindl1 and Reindl2 calculate the diffuse fraction K_d while Maxwell, Lopez and Louche calculate the solar direct transmittance K_b..

a) Reindl1 Model

$$K_d = 1.020 - 0.248K_T \qquad K_T \leq 0.30$$
$$K_d = 1.450 - 1.670K_T \qquad 0.30 < K_T < 0.78 \qquad (7)$$
$$K_d = 0.147 \qquad K_T \geq 0.78$$

b) Erbs Model

$$K_d = 1.0 - 0.09K_T \qquad K_T \leq 0.22$$
$$K_d = 0.9511 - 0.1604K_T + 4.388{K_T}^2 - 16.638{K_T}^3 + 12.336{K_T}^4 \qquad 0.22 < K_T \leq 0.8 \qquad (8)$$
$$K_d = 0.165 \qquad K_T > 0.8$$

c) Reindl2 Model

$$K_d = 1.020 - 0.254K_T + 0.0123\, sin\alpha \qquad K_T \leq 0.30$$
$$K_d = 1.400 - 1.749K_T + 0.177\, sin\alpha \qquad 0.30 < K_T < 0.78 \qquad (9)$$
$$K_d = 0.486K_T - 0.182\, sin\alpha \qquad K_T \geq 0.78$$

d) Maxwell Model

$$K_b = K_{nc} - (A + B\exp(mC)) \qquad (10)$$

Where

$$K_{nc} = 0.866 - 0.122\, m + 0.0121\, m^2 - 0.000653\, m^3 + 0.000014\, m^4 \quad (11)$$

m is the relative optical mass obtained by [30]:

$$m = \left({}^{p}/_{p_0}\right)(cos\theta + 0.15 * (93.885 - \theta)^{-1.253})^{-1} \qquad (12)$$

The correction pressure factor is given by:

$$\frac{p}{p_0} = \exp\left(\frac{-z}{8435.2}\right) \qquad (13)$$

z is the altitude over the sea level

A, B, C are coefficients given by:

For $K_T \leq 0.6$:

$$A = 0.512 - 11.56\,K_T + 2.286\,{K_T}^2 - 2.222\,{K_T}^3$$
$$B = 0.370 + 0.962\,K_T \qquad (14)$$
$$C = -0.280 + 0.932\,K_T - 2.048\,{K_T}^2$$

for $K_T > 0.6$:

$$A = -5.743 + 21.77\,K_T - 27.49\,{K_T}^2 + 11.56\,{K_T}^3$$
$$B = 41.40 - 118.5\,K_T + 66.05\,{K_T}^2 + 31.90\,{K_T}^3 \qquad (15)$$
$$C = -47.01 + 184.2\,K_T - 222.0\,{K_T}^2 + 73.81\,{K_T}^3$$

e) Lopez Model

$$K_b = (0.928 - 0.909\,cos\theta){K_T}^2 \qquad K_T \leq 0.325 \qquad (16)$$
$$K_b = 0.069 - 0.475\,K_T + 1.733\,{K_T}^2 - 0.096\,cos\theta \qquad K_T > 0.325$$

$\theta=\pi/2-\alpha$ is the solar zenith angle.

f) Louche Model

$$K_b = 0.002 - 0.059K_T + 0.994{K_T}^2 - 5.205{K_T}^3 + 15.307{K_T}^4 - 10.626{K_T}^5 \qquad (17)$$

4. Analysis of models performance to estimate hourly values

Models described in section 3 have been applied to data from nine locations, presented in Table I, to estimate direct and diffuse solar irradiance firstly on an hourly basis. To evaluate the models performance, estimated, E_i, and measured, M_i, values have been compared by means of two classical statistical indicators, the root mean square error (*RMSE*) and the mean bias error (*MBE*) whose absolute (W/m^2) and relative (%) values are defined by eqs. (18) and (19) respectively [34]:

$$RMSE = \sqrt{\frac{1}{N_I}\sum_{i=1}^{N}(E_i - M_i)^2} \qquad RMSE(\%) = \frac{100}{\langle M_i \rangle}RMSE \qquad (18)$$

$$MBE = \frac{1}{N}\sum_{i=1}^{N}(E_i - M_i) \qquad MBE(\%) = \frac{100}{\langle M_i \rangle}MBE \qquad (19)$$

where ‹M_i› is the mean value of the measured values sample for each particular hour in each day of the month and *N* is the number of data points.

In Section 4.1, the models performance is analyzed by considering the whole data available for each location (overall performance) while in Sections 4.2 and 4.3 a more detailed analysis is made by considering different ranges of K_T and α.

4.1 Overall performance

The performance analysis results are shown in the graphs of the Figure 1; each graph shows the relative RMSE (%) for the direct B_h and diffuse D_h solar irradiances for each model. Locations are indicated by letters: S (Santander), O (Oviedo), LE (León), VA (Valladolid), LL (Lleida), SA (Salamanca), M (Madrid), CC (Cáceres) and MU (Murcia).

Figure 1. *RMSE values for the direct B_h and diffuse D_h solar irradiances obtained from six models and nine locations in Spain*

Results from Figure 1 show that the relative RMSE is higher for the diffuse component than for the direct one and that, for a specific component and location, there are no significant differences among models; concerning B_h, Santander and Oviedo, with abundant number of cloudy days, present the worst performance while Lleida is in the opposite case. The highest errors are obtained for Santander and Louche (RMSE=33.7%, MBE=17.7%) and the lowest for Lleida and Erbs (RMSE=16.0%, MBE=0.2%). Based on the climate, the highest performance is for *Bsk* (16-18%) followed by *Csa* (17.7-18.4%), *Bsh* (17.7-22%), *Csb* (19.4-27.8%) and *Cfb* (25.8%-33.7%). Concerning D_h, RMSE exceeds 30% in all cases, the highest errors correspond to Caceres and Reindl2 (RMSE=47.0%, MBE=21.6%) and the lowest to Murcia and Lopez (RMSE=32.0%,MBE=-3.7%). RMSE and MBE errors for all combinations model-location are reported in Appendix A for the direct (Table A.I) and the diffuse (Table A.II) irradiances.

The results obtained in the Figure 1 are consistent with the results of previous studies in the literature, which mostly use hourly data. In the next subsections, an analysis of models performance by sorting data in different ranges of K_T and α is carried out.

4.2 Performance of models for different ranges of K_T

Performance of models for different clearness index K_T ranges, that is, for different cloudiness conditions is analyzed here. It have been considered those K_T ranges established by authors in their original formulation (eqs. 7-17); three K_T ranges have been taken for Erbs, Reindl1 and Reindl2 models and two ranges of K_T for Maxwell and Lopez models; Louche model does not differentiate among ranges of K_T, however, performance in the same two ranges as Lopez model has been studied. Results obtained show that, in the case of the direct component B_h, all models present high values of RMSE for cloudy skies (low K_T) which decrease significantly for clear skies (high K_T). In the case of the diffuse component D_h, the behavior is the opposite; Figure 2 shows RMSE values for the Erbs model, taken as an example, for the nine studied locations and for three ranges of K_T given in eq. (8) where K_1, K_2 and K_3 correspond to cloudy, intermediate and clear skies, respectively.

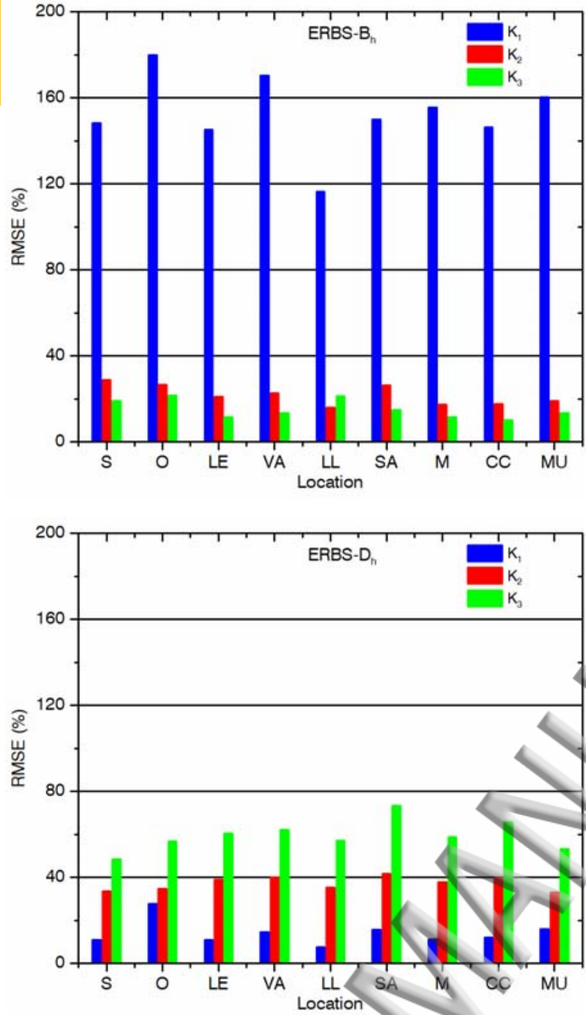

Figure 2. . *RMSE values for a) direct and b) diffuse solar irradiances obtained from the Erbs model for nine locations and three K_T-ranges*

RMSE values shown in the Figure 2 are relative errors (in %) respect to the mean solar irradiance for each K_T interval (eq. 18). Absolute errors are similar for both components, for example, for Erbs model and Madrid, in the case of B_h, the absolute errors for the ranges K_1, K_2 and K_3 are 10.2, 54.3, 79.2 W/m^2, respectively while the corresponding errors for D_h are 11.4, 51.4, 77.4 W/m^2; the high differences found in the relative errors are due to the different magnitude that present the direct and the diffuse radiation depending on the cloudiness condition. The analysis reported for Erbs model can be applied to the rest of models.

In the case of models with two K_T ranges the behavior is similar; Figure 3 shows the results for the Lopez model as an example; K_1 and K_2 correspond to cloudy and clear skies respectively; high RMSE values, more than 100%, are obtained for B_h in the case of cloudy skies as said above due mainly to the low magnitude of B_h for this type of sky; Lower errors of 29.6% and 16.2% for

Santander and Lleida, respectively, are obtained for clear skies. For D_h, the behavior is the opposite as already commented for Figure 2. RMSE and MBE values for all combinations model-location are reported in Appendix B (Table B.I)

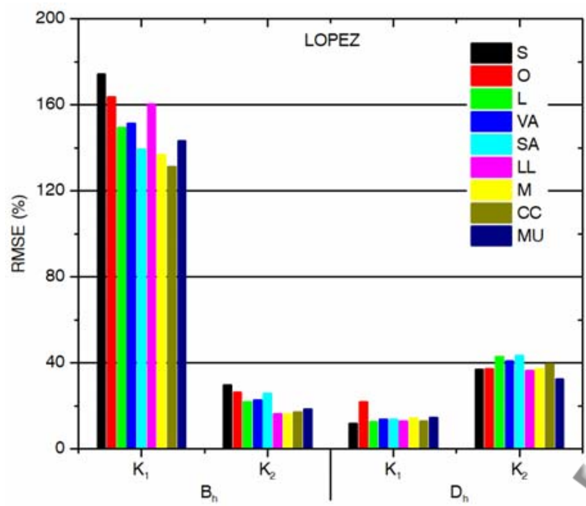

Figure 3. *RMSE values for direct and diffuse irradiances for nine locations and two K_T ranges corresponding to the Lopez model*

4.3 Performance of models for different ranges of solar altitude

The models performance for different intervals of the solar altitude angle, α, is analyzed in this section. Four ranges for α have been taken: α<20º, 20º-40º, 40º-60º and α>60º. While for the diffuse component D_h, RMSE values are similar for all models and all α-ranges, errors depend significantly on α in the case of the direct component B_h: RMSE decrease when α increases for all models. Table II shows the RMSE values for both components, all models for Murcia as an example. The rest of locations present similar results.

Table II. *RMSE values obtained from the six studied models, four solar altitude angle ranges and for the direct B_h and diffuse D_h solar irradiancies (Murcia)*

	B_h				D_h			
α (°)	<20	20-40	40-60	>60	<20	20-40	40-60	>60
Reindl1	33.5	18.8	15.8	14.1	38.8	33.9	29	29.5
Erbs	34.4	17.9	16.5	15.3	40	31	29.6	32.1
Reindl2	30.3	18.1	15.3	13.1	33	32.2	31.1	32.4
Maxwell	35.3	20.4	15.3	13.4	31.9	31.3	28.5	34.2
Lopez	31.6	19.5	16.5	13.9	31.6	31.6	29.5	29

Louche	31.3	19.1	19.4	18.5	34.7	30.4	33.9	38.5

Figure 4 shows another example, RMSE values for Oviedo and Louche model. It can be seen that errors for D_h present a small variation from 33.9% to 37.2% while for B_h, the variation is from 42.1% for $\alpha < 20°$ to 24.1% for $\alpha > 60°$. RMSE and MBE errors for all combinations model-location are reported in Appendix B (Tables B.II and B.III).

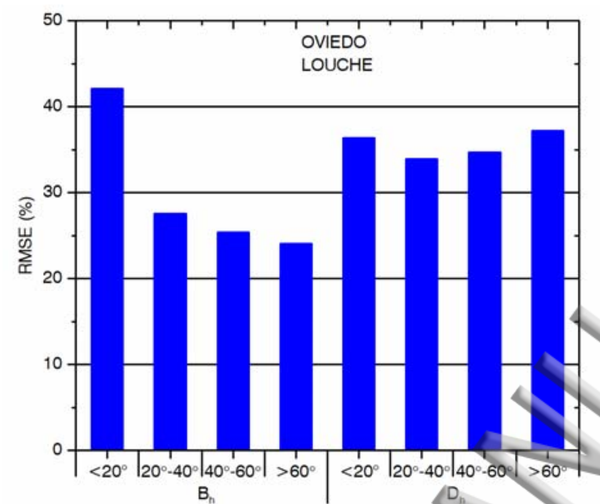

Figure 4. *RMSE values for the direct and diffuse irradiances obtained from Louche model for Oviedo.*

Conclusions from the analysis carried out in section 4 are that decomposition models estimating direct and diffuse horizontal solar irradiance on an hourly basis have a performance which depends on the sky condition and on the solar altitude angles. Figure 1 gives the overall performance, that is, by considering all type of data, results that are usually reported in the literature. More realistic are the Figures in subsections 4.2 and 4.3 which provide numerical values of errors that allow to decide in each particular situation where such models can be used and establish the corresponding errors that should be assumed. Finally, no discernible improvement can be appreciated between models that calculate K_d or K_b neither between univariate or bivariate models.

5. Performance of models to estimate Monthly Average Hourly values

In our previous analysis, it has been shown that, on an hourly basis, decomposition models do not offer an adequate accuracy to represent the behavior of the solar radiation components for all solar altitudes and cloudiness conditions. By other side, it is assumed that the use of several type of averaged values will improve performance. Averaged radiation values representing the climate of a specific geographical area can be useful in applications as managing the efficient use of a solar energy installation [35-37] or carrying out climatic studies [38]. It will be shown that decomposition models can be applied in such cases to provide climatic values of direct and diffuse solar irradiance in locations where only the global one is measured. In this analysis, specifically, monthly average hourly (MAH) values have been chosen; the database was arranged so that all data available for a single month and a single hour, irrespective of the year, were utilized to determine a monthly mean hourly value [26, 39]. It will be assumed that the long-term average irradiation calculated from experimental data is not significantly different from the true climatological value [11].

The annual evolution of MAH values for global, direct and diffuse measured irradiances is represented in Figure 5a for Madrid taken as an example while in Figure 5b the direct component B_h is shown for five out of nine locations. Values from sunrise to sunset are represented. The other components and locations present a similar behavior; a smooth evolution can be observed from both Figures in which irradiance values, elaborated from experimental data, include all sky types.

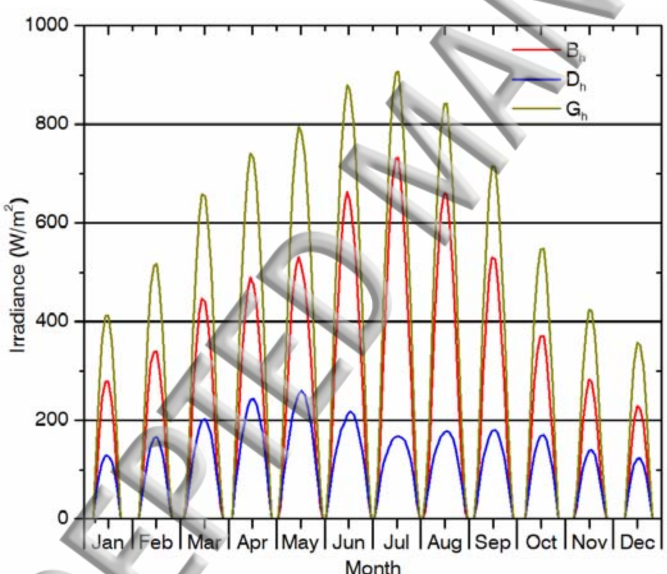

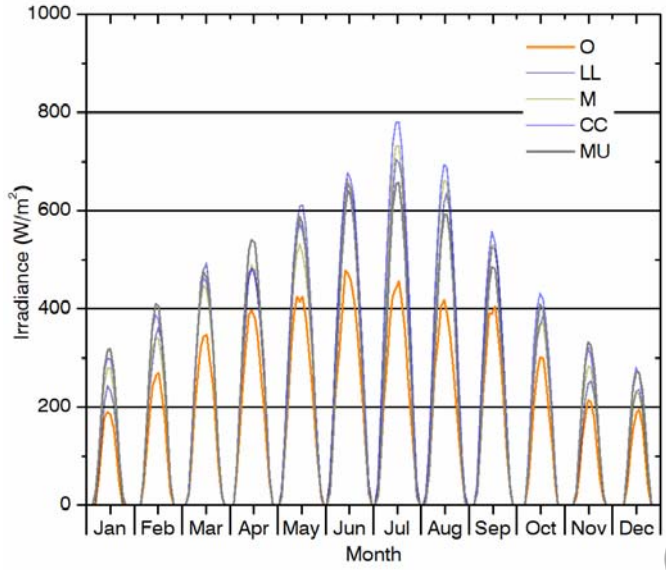

***Figure 5**. a) Annual evolution of the monthly average hourly values of global G_h, diffuse D_h and direct B_h irradiances for Madrid obtained from measurements, b) Annual evolution of the monthly mean hourly direct irradiance B_h for five locations in Spain obtained from measurements.*

A performance analysis similar to that carried out in section 4 for hourly values is done in the present section for a different time basis consisting in using MAH data; thus, an analysis of errors RMSE and MBE obtained for six models and nine locations has been also carried out. Figure 6 shows a comparison between RMSE values obtained from MAH and hourly (H) values for all locations and both components B_h and D_h for Erbs model taken as an example. From this figure, the decrease of the errors when considering MAH values is significant for both components which support the idea that the use of MAH values is a time basis better than hourly values for the application of decomposition models; Figure 6 shows that for B_h, RMSE for MAH values vary between 6.4% and 16.3% corresponding to Lleida and Oviedo respectively; for D_h the variation is 17.3% and 23.3% for the same locations.

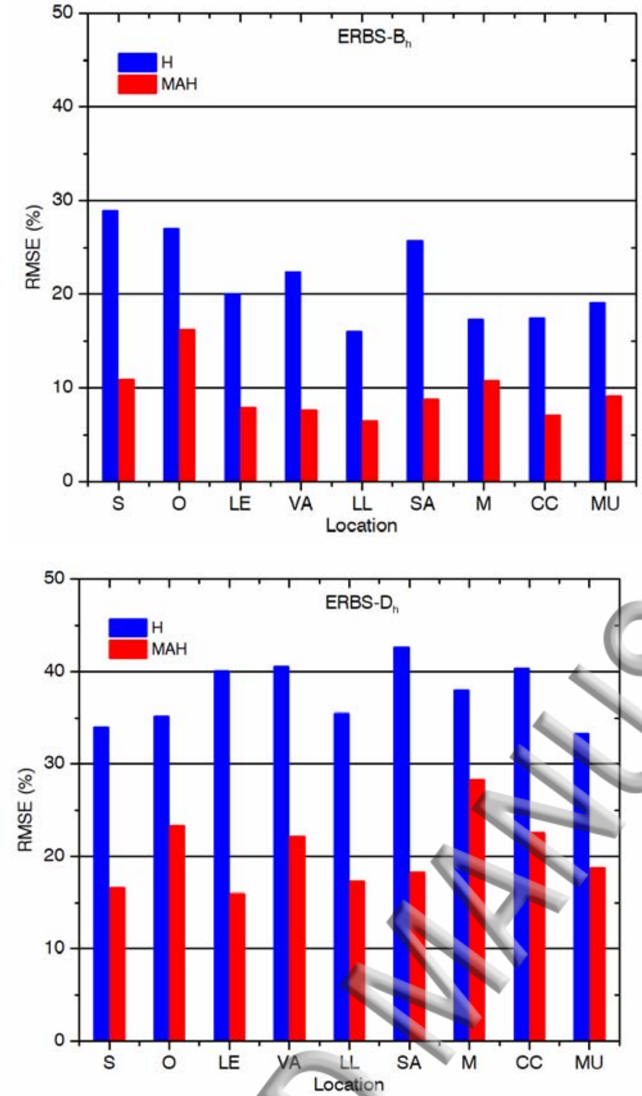

Figure 6. *RMSE values for hourly (H) and monthly average hourly (MAH) values for a) the direct B_h and b) diffuse D_h solar irradiances for all locations and for Erbs model*

6. Proposal of a K_d-K_T algorithm to estimate Monthly Average Hourly values

Having into account the utility of decomposition models to estimate MAH values, a new algorithm is proposed in this section, which summarizes the main analyzed relationships K_d=f(K_T, α) with the aim to be applied to a wide area in Spain. A preliminary study on the relationship between B_h and K_T can be found in Perez-Burgos et al. [40]. Data described in Table I have been used in this study divided in two data samples; five locations, Oviedo, Lleida, Madrid, Caceres and Murcia have been used to develop the algorithm and the other four, Santander, Leon, Valladolid and Salamanca have been used for validation. MAH values of global, direct and diffuse solar irradiances have been calculated for the whole data set and for each location. The averaged values of global irradiance have been used to calculate averaged values of the clearness index K_T by using the eq. (1). By considering the main relationships found in the models studied in the section 3, a regression analysis over the experimental data has been carried out . The following expression has been obtained with a correlation coefficient R=0.94.

$$K_d = 0.703 + 0.427K_t - 1.781K_t^2 + 0.178\, sin\alpha \qquad (20)$$

where K_d and K_T are the monthly average hourly values of the diffuse fraction and clearness index respectively and α is the solar altitude angle for the 15th day of each month.

6.1 Validation of the proposed algorithm

The estimated values of K_d by eq. (20) have been used to estimate MAH values of the diffuse and direct irradiances following the steps described in section 3. Estimated and experimental values are compared in Figure 7. This figure shows that the proposed algorithm fits in a high precision to the experimental data for the direct irradiance and to a lesser extent for the diffuse one.

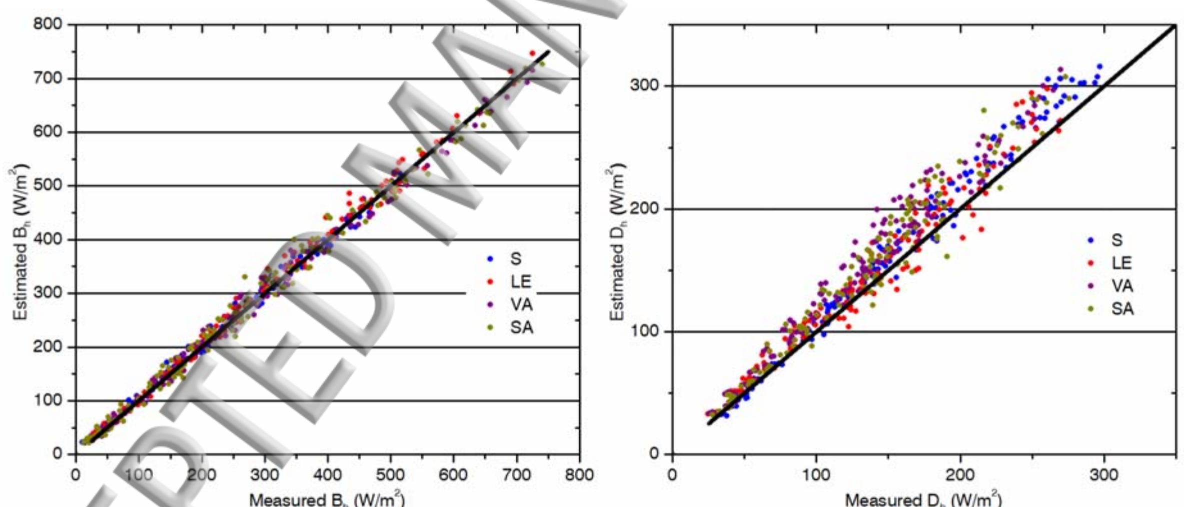

Figure 7*. Comparison between monthly average hourly values, experimental and estimated by Equation (20), for a) the direct B_h and b) the diffuse D_h solar irradiances. Line 1:1 is represented in both graphs.*

In Figure 8, the annual evolution of the estimated and experimental MAH values for the direct solar irradiance is shown for each one of the four validation locations.

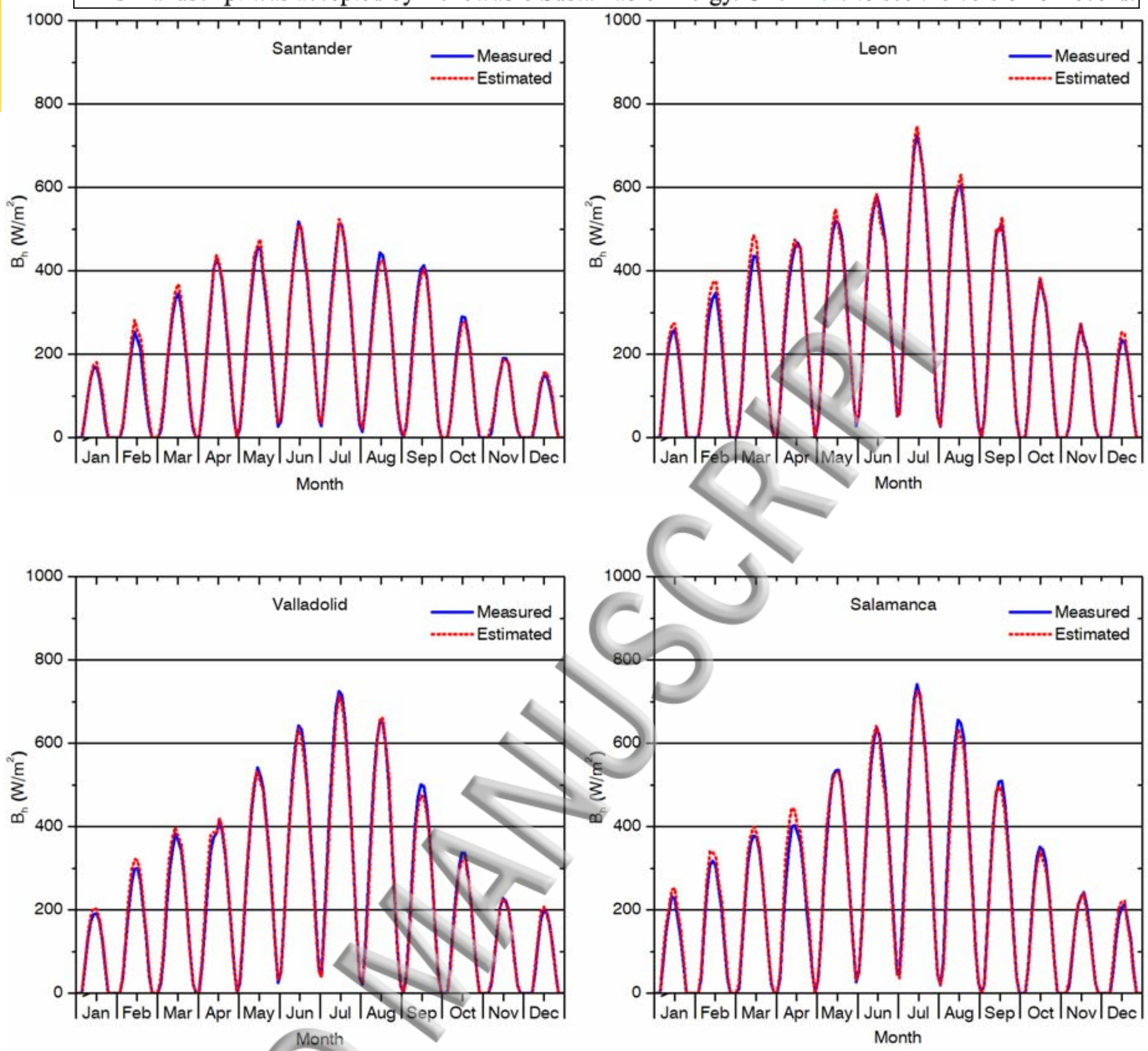

Figure 8. *Annual evolution of the monthly average hourly values of direct irradiance for the four locations used in the validation process. Curves obtained from measured and estimated values are compared.*

Estimated and experimental curves fit very well in general. During the winter months, the predicted results were characterized of overestimation when compared to the measured data with difference less than 10%; The best performance of the model is obtained for summer time where predictions should be more useful due to the high level of available solar radiation. The maximum values of direct radiation, obtained in July at noon, are 517.4, 582.5, 642.7 and 638.5 W/m^2 for Santander, Leon, Valladolid and Salamanca respectively; these values are predicted by the model with relative differences of 1.7, -0.2, 0.9 and -0.5 %; these low differences indicate the good accuracy of the model.

Figure 9 shows a comparison between RMSE values obtained from the Reindl2 model and the proposed algorithm to evaluate the differences in performance between both of them; RMSE is reduced by 3% and 12% for B_h and D_h respectively. Table III shows numerical values of RMSE and MBE obtained with the proposed algorithm for the four locations used for validation; for D_h, RMSE varies from 10.4 to 18.9% and MBE is below 16%. For B_h, percentage errors are considerably lower so that RMSE varies from 5.0 to 6.2% and MBE is below 1.6%. These low errors indicates that the algorithm given by eq.(20) improves the performance over the analyzed models and presents a high accuracy, mainly, to reconstruct climatic monthly average hourly values of the direct irradiance in Spain.

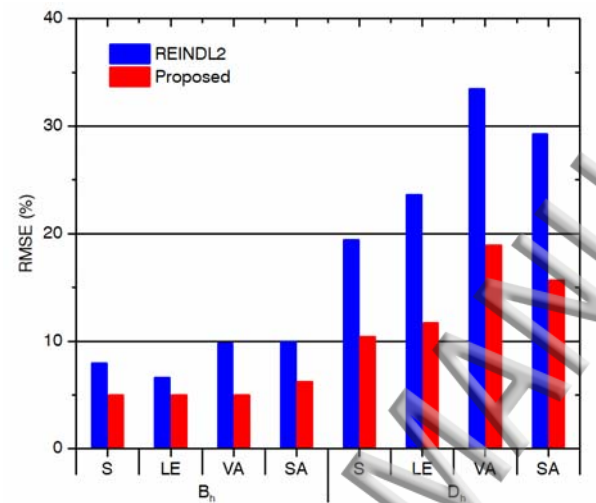

Figure 9. *Comparison between RMSE values obtained by the proposed algorithm (eq. 20) and the Reindl2 model for the direct and diffuse irradiances and for the four locations used in the validation process.*

Table III. *RMSE(%) and MBE(%) obtained for the four locations used to validate the proposed algorithm.*

	S	LE	VA	SA
RMSE B_h	5.0	5.0	5.0	6.2
MBE B_h	-1.6	0.2	0.2	-0.6
RMSE D_h	10.4	11.7	18.9	15.7
MBE D_h	-7.1	4.3	-15.9	-10.8

7. CONCLUSIONS

Determining the solar radiation components, direct and diffuse, is essential in design and performance studies of several solar energy applications. Radiation modeling is an important factor in the evaluation of solar energy resources in radiometric stations where no experimental data are available. This paper deals with the performance assessment of solar radiation decomposition models, which estimates the direct and diffuse solar radiation from the global one. High quality, long-term data of global, direct and diffuse solar irradiance provided by the National Meteorological Agency (AEMET) from nine locations in Spain have been managed in this work. An in-depth analysis has been carried out with the aim to evaluate the performance of six well-known decomposition models, firstly, on hourly basis and, subsequently, on monthly average hourly basis. The analysis based on hourly data show that the model performance depends significantly on the clearness index K_T and the solar altitude angle α. In the case of the direct irradiance, B_h, the lowest relative errors are obtained for clear days (high K_T) and high solar altitude angles. For the diffuse component D_h, the behavior is the opposite with respect to K_T while α has no influence on the performance. By other hand, for a specific location, no remarkable differences have been appreciated among models.

The same models have been used to estimate monthly average hourly (MAH) values so that results show an increase of the performance with respect to that obtained for hourly values; this result has been valued positively in spite of the loss of time-resolution over the hourly data due to MAH data are very useful in many solar applications.

Finally, a decomposition algorithm has been proposed by the expression (20) to estimate MAH values of direct and diffuse solar irradiances with a correlation coefficient of R=0.94. The proposed algorithm improves the estimations of the analyzed models; the interest of such estimations is to reconstruct climatic monthly average hourly values of direct and diffuse solar irradiance in locations where only global one is available.

ACKNOWLEDGEMENTS

This work was supported by grants from both the Spanish Government (ENE2014-54601R) and the Regional Government of Castile and Leon (BU358A12-2). The authors wish to thank the National Meteorological Agency in Spain (AEMET) for supplying the data used in this work.

Appendix A. Overall models performance: Tables

Table A.I. *Values of RMSE and MBE (absolute value in W/m² and percentage) obtained from the comparison between estimated and measured data of direct solar irradiance, B_h, on hourly basis for six models and nine locations.*

B_h		REINDL1		ERBS		REINDL2		MAXWELL		LOPEZ		LOUCHE	
		RMSE	MBE	RMSE	MBE	RMSE	MBE	RMSE	MBE	RMSE	MBE	RMSE	MBE
S	W/m²	68.4	24.2	68.9	24.6	61.4	13.7	66.1	30.7	74.8	38.2	80.2	42.3
	(%)	28.7	10.2	28.9	10.3	25.8	5.8	27.8	12.9	31.4	16	33.7	17.7
O	W/m²	63	3.3	63.1	3.5	62.3	-5.1	65.1	6.9	66.2	16.5	68.2	20.3
	(%)	27	1.4	27	1.5	26.7	-2.2	27.9	3	28.3	7.1	29.2	8.7
LE	W/m²	59.8	14.9	61.1	14.6	59.3	1.6	60.2	18.7	69.5	33.9	71.1	34.8
	(%)	19.5	4.9	20	4.8	19.4	0.5	19.7	6.1	22.7	11.1	23.2	11.4
VA	W/m²	67.6	8.3	68.5	10	68.3	-2.5	72	9.3	71.8	23.5	75.7	29.4
	(%)	22.1	2.7	22.4	3.3	22.3	-0.8	23.5	3	23.5	7.7	24.7	9.6
SA	W/m²	77.8	10.3	79.1	10.8	78.4	-1.8	80.2	10.7	82.2	26.5	85.6	30.7
	(%)	25.3	3.3	25.7	3.5	25.5	-0.6	26	3.5	26.7	8.6	27.8	10
LL	W/m²	52	-4.6	50.8	0.5	55.1	-12.3	57	6.5	52.7	9.3	55.4	18.6
	(%)	16.4	-1.5	16	0.2	17.4	-3.9	18	2.1	16.7	2.9	17.5	5.9
M	W/m²	55.6	-15.3	54.3	-12	60	-24.5	61.5	-13.9	53.4	-1.2	54.9	6.2
	(%)	17.7	-4.9	17.3	-3.8	19.1	-7.8	19.6	-4.4	17	-0.4	17.4	2
CC	W/m²	59	-6.5	59.1	-4.1	62.8	-17.6	61	1.5	59.8	9	62.5	15.9
	(%)	17.3	-1.9	17.4	-1.2	18.5	-5.2	17.9	0.4	17.6	2.6	18.4	4.7
MU	W/m²	57.2	5	59	9.9	54.6	-4.9	57.2	13.3	58.4	18.2	68	28.5
	(%)	18.5	1.6	19.1	3.2	17.7	-1.6	18.5	4.3	18.9	5.9	22	9.2

Table A.II. *Values of RMSE and MBE (absolute value in W/m² and percentage) obtained from the comparison between estimated and measured data of diffuse solar irradiance, D_h, on hourly basis for six models and nine locations.*

Dh		REINDL1		ERBS		REINDL2		MAXWELL		LOPEZ		LOUCHE	
		RMSE	MBE	RMSE	MBE	RMSE	MBE	RMSE	MBE	RMSE	MBE	RMSE	MBE
S	W/m2	58.6	-8.3	58.6	-8.7	56.1	2.1	55.4	-14.9	62	-22.3	66.2	-26.4
	(%)	34	-4.8	34	-5.1	32.6	1.2	32.2	-8.6	36	-13	38.5	-15.4
O	W/m2	59.1	0.3	59.4	0	58.9	8.6	60.4	-3.4	61.3	-13	63.7	-16.8
	(%)	35	0.2	35.2	0	34.8	5.1	35.8	-2	36.3	-7.7	37.7	-9.9
LE	W/m2	54.8	0.4	56.5	0.6	61.7	13.6	55.1	-3.5	58.6	-18.7	60.7	-19.5
	(%)	38.8	0.3	40.1	0.4	43.8	9.6	39.1	-2.5	41.6	-13.3	43.1	-13.9
VA	W/m2	57.3	13	56.9	11.2	63.9	23.8	63.1	12	56	-2.2	57.2	-8.2
	(%)	40.9	9.2	40.6	8	45.6	17	45.1	8.5	40	-1.6	40.8	-5.8
SA	W/m2	60.8	6.7	61.7	6.1	67.8	18.7	67	6.2	61.5	-9.6	63.5	-13.8
	(%)	42	4.6	42.6	4.2	46.8	12.9	46.3	4.3	42.5	-6.6	43.8	-9.5
LL	W/m2	52.5	11.2	50.4	6.1	56.4	18.9	54.8	0.1	50.9	-2.7	52.7	-12

	(%)	36.9	7.9	35.5	4.3	39.7	13.3	38.5	0	35.8	-1.9	37.1	-8.4
M	W/m2	52.9	21.3	51.5	18	59	30.5	60.5	19.9	49.1	7.2	49.8	-0.3
	(%)	39.1	15.7	38	13.3	43.5	22.5	44.6	14.7	36.2	5.3	36.7	-0.2
CC	W/m2	53.7	17.4	53.4	14.9	62.1	28.4	56.3	9.3	50.7	1.9	52.1	-5
	(%)	40.7	13.2	40.4	11.3	47	21.6	42.7	7.1	38.5	1.4	39.5	-3.8
MU	W/m2	51	7.4	51.4	2.6	52.4	17.4	51.1	-0.9	49.4	-5.7	56.6	-16
	(%)	33.1	4.8	33.3	1.7	34	11.3	33.2	-0.6	32	-3.7	36.7	-10.4

Appendix B. Model performance for different ranges of K_T and α:Tables

Table B.I. *Values of RMSE and MBE (in percentage) obtained from the comparison between estimated and measured data of direct, B_h, and diffuse, D_h, solar irradiances on hourly basis for six models and nine locations by considering different clearness index ranges.*

		DIRECT B_h						DIFUSSE D_h					
		RMSE (%)			MBE (%)			RMSE (%)			MBE (%)		
		K_1	K_2	K_3	K_1	K_2	K_3	K_1	K_2	K_3	K_1	K_2	K_3
S	REINDL1	139.9	28.6	21.1	-53.2	9.8	17.8	10.2	33.6	52.7	5.5	-4.4	-34.8
	ERBS	148.4	29	19.2	-69.9	10.1	15.3	10.9	33.7	48.4	6.5	-4.8	-26.8
	REINDL2	241.9	26.2	11	-164.6	6.2	-0.8	16.8	32.3	46	12.2	0.6	24.9
	MAXWELL	73.1	19.5	-	30.1	10.2	-	22.2	43.1	-	-5	-13.3	-
	LOPEZ	174.3	29.6	-	89.7	15.7	-	11.7	37.1	-	-3.8	-13.8	-
	LOUCHE	154.7	31.8	-	39.1	17.7	-	10.9	39.6	-	-0.3	-16.8	-
O	REINDL1	175.6	26.6	23.1	-80.9	1.1	16.9	27.1	34.4	61	13	0.5	-40.6
	ERBS	179.8	26.7	21.5	-87.7	1.3	14.4	27.8	34.7	56.8	14.1	0.2	-33.3
	REINDL2	221.6	26.6	15.5	-131.4	-2	-0.5	34.4	34.6	46.2	21	4.8	10.7
	MAXWELL	63.2	19	-	-0.7	3.8	-	26.3	48.5	-	1.7	-7.6	-
	LOPEZ	163.7	26.5	-	-8.8	7.2	-	22	37.2	-	1.9	-8.8	-
	LOUCHE	154.1	27.3	-	-27	9.1	-	20.8	38.8	-	4.4	-11.5	-
LE	REINDL1	135.5	20.5	12.4	-59.3	4.7	5.8	10.3	37.7	58.4	5.1	0.2	0.4
	ERBS	145.3	21.1	11.6	-74.6	5	3.5	11.1	38.9	60.5	6.3	-0.3	12.7
	REINDL2	242.9	20.1	12.9	-164.9	1.9	-7.4	18.5	39.9	92.3	12.9	5.9	72.9
	MAXWELL	57.5	15.6	-	10.3	5.7	-	24.8	49.6	-	-1.3	-3.4	-
	LOPEZ	149.4	22	-	51.4	11	-	12.6	42.8	-	-3.3	-13.9	-
	LOUCHE	128.7	22.6	-	16.8	11.3	-	11.2	44.3	-	-0.4	-14.7	-
VA	REINDL1	163.6	22.4	13.9	-58.5	2.6	5.3	14	40.5	59.2	7.2	9.4	4.2
	ERBS	170.3	22.7	13.4	-73.6	3.3	3.1	14.6	40.2	62.3	8.2	7.8	16.9
	REINDL2	243.8	22.6	14.4	-153.1	-0.5	-7	20	44.3	94.2	13.9	15.8	75.1
	MAXWELL	57.5	18.7	-	8.1	2.5	-	27.3	58.9	-	2.7	13.8	-
	LOPEZ	151.3	22.8	-	46.6	7.6	-	13.9	41	-	-2	-1.6	-
	LOUCHE	134.2	24	-	9.8	9.6	-	12.8	41.9	-	1.4	-6.3	-
SA	REINDL1	144.7	26	15	-71	3.3	3.8	15	41.2	68.8	8	4.4	10.9
	ERBS	149.9	26.5	14.8	-81.7	3.7	1.6	15.6	41.7	73.3	9.1	3.6	24.5
	REINDL2	201.8	26	16.8	-140.3	0.2	-8.6	21.5	44.5	110.2	15.2	10.8	87.9
	MAXWELL	68.4	20.4	-	6	3.2	0	29.8	59.5	-	2	6.3	-
	LOPEZ	139.4	25.9	-	28.1	8.6	-	13.7	43.5	-	-2.2	-6.9	-
	LOUCHE	135.1	27	-	-5.5	10	-	13.3	44.9	-	1.3	-10.2	-
LL	REINDL1	110.9	16.3	23	-51.4	-1.6	17.6	7	36.7	61.3	4.3	8.2	-38.9
	ERBS	116.4	15.9	21.3	-69.5	0	15.1	7.5	35.3	57.2	5.4	4.5	-31.4
	REINDL2	215.5	17.4	14.3	-166	-3.9	0.8	13.6	39.6	48	11.2	13.3	12

	MAXWELL	49.1	14.4	-	16.4	0.6	-	23.5	47.7	-	-5.9	4.3	-
	LOPEZ	160.4	16.2	-	63.5	2.8	-	12.9	36.5	-	-4	-1.8	-
	LOUCHE	145.7	17.1	-	25	5.8	-	12.2	37.8	-	-1	-8.8	-
M	REINDL1	147.4	17.7	11.5	-56.5	-5.1	3	10.5	38.9	57.8	5.3	16.1	-6.2
	ERBS	155.6	17.3	11.4	-72	-3.9	0.8	11.2	37.8	58.7	6.3	13.4	5.2
	REINDL2	253.8	19	14.4	-174.4	-7.7	-9.6	17.7	42.9	81.8	12.9	22.1	60.4
	MAXWELL	45.7	15.2	-	-4.8	-4.4	-	28.8	56	-	7.6	20.8	-
	LOPEZ	136.9	16.4	-	25.2	-0.5	-	14.2	37.3	-	-0.5	5.7	-
	LOUCHE	122.9	16.8	-	-4.5	2	-	13.1	37.9	-	2.5	-0.4	-
CC	REINDL1	138.6	17.7	10.2	-63.5	-2.2	2.5	11.3	40.3	60	5.8	13.2	14.4
	ERBS	146.4	17.7	10.1	-76.9	-1.3	0.3	12.1	39.9	65.9	6.9	11	28.4
	REINDL2	227.7	18.6	13.4	-158.3	-4.9	-9.3	19.2	45.2	107.4	13.5	20.1	91
	MAXWELL	51.4	14.3	-	3.6	0.1	-	27.4	52.9	-	2.2	10.7	-
	LOPEZ	131.2	17.1	-	26.6	2.6	-	12.9	39.5	-	-1.4	1.6	-
	LOUCHE	125.1	17.9	-	5.8	4.7	-	12.3	40.5	-	0.6	-4	-
MU	REINDL1	154.3	18.5	14.4	-66.9	1.5	7.8	15.2	32.9	55.3	7.7	5	-19.2
	ERBS	160.4	19.1	13.4	-78.9	3.2	5.5	15.9	33.1	53.3	8.7	1.7	-9.3
	REINDL2	230.9	17.6	13	-151.8	-1.5	-5.4	22.1	33.6	63.3	15.2	11	38.1
	MAXWELL	47.9	14.4	-	10.9	3.5	-	24.4	38.4	-	-0.8	-0.4	-
	LOPEZ	143.2	18.4	-	36.3	5.8	-	14.6	32.5	-	-1.9	-3.8	-
	LOUCHE	127.2	21.4	-	1.2	9.2	-	13.5	37.3	-	1.6	-10.9	-

Table B.II. *Values of RMSE and MBE (in percentage) obtained from the comparison between estimated and measured data of direct solar irradiance,* B_h*, on hourly basis for six models and nine locations by considering different solar altitude angle ranges.*

α(º)		DIRECT B_h							
		RMSE (%)				MBE (%)			
		<20	20-40	40-60	>60	<20	20-40	40-60	>60
S	REINDL1	40.4	27.7	24	23.9	0	7.7	12.1	13.3
	ERBS	41.5	27.4	24.2	24.4	-2.9	8.4	12.5	13.2
	REINDL2	41.1	26.2	21.3	20.5	8.9	7.2	5.3	3.4
	MAXWELL	51.9	32.6	22	18.2	29.8	19.1	10.2	3
	LOPEZ	48.8	34.5	25.5	23.2	23.2	18.4	14.7	12.7
	LOUCHE	42.7	31.3	28.6	28.5	7.1	15.8	19.7	20.3
O	REINDL1	41.7	26.8	22.7	21.8	-6.9	-0.8	4.3	3
	ERBS	43	26.2	22.9	22.2	-9.4	-0.2	4.6	2.7
	REINDL2	40.3	25.9	22.2	22.7	1.3	-0.2	-2.4	-7.1
	MAXWELL	46.2	28.2	22.1	23.9	19.5	9.5	-0.3	-10.5
	LOPEZ	45.7	29	23.6	22.1	14.7	8.7	6.5	1.8
	LOUCHE	42.1	27.6	25.4	24.1	-0.2	6.9	11.6	9.6
LE	REINDL1	27.9	19.2	16.6	15.6	-5.2	4.3	6.8	6
	ERBS	27.9	19.1	17.1	16.3	-4.6	5.3	6.1	4.8
	REINDL2	26.9	19.1	16.4	15.7	3.3	3.9	-1.1	-3.7
	MAXWELL	32.3	22	15.2	14.6	19.2	12.5	3.1	-5.1
	LOPEZ	31	23.6	19.3	16.8	11.7	12.8	10.8	8.2
	LOUCHE	28	22.1	20.2	19	2.4	11.6	12.8	11.6
VA	REINDL1	37.6	25.3	19.1	14	-7.8	2.9	4.3	2.7
	ERBS	38.6	25.1	19.3	14.7	-9.1	4.4	4.9	2.4
	REINDL2	35.8	25.3	18.9	15.2	0.6	3.8	-1.6	-5.8
	MAXWELL	41.3	28	18.5	16.6	19.3	12.8	0.3	-9.2
	LOPEZ	39.9	27.9	20.2	14.2	10.9	11.4	7	3.3
	LOUCHE	37.8	27.3	21.7	16.4	-1.1	10.8	11.1	8.5
SA	REINDL1	40.8	27.2	21.9	17.5	-6	2.9	5	3.7

	ERBS	41.5	27.2	22.2	18.2	-7	4	5.1	3.1
	REINDL2	39.1	27.2	21.9	18.2	1.8	3.3	-1.5	-5.1
	MAXWELL	44.1	29.6	21.2	18.6	18.3	11.8	1	-7.9
	LOPEZ	45.2	29.9	22.9	17.6	12.6	11.4	8	4.7
	LOUCHE	41	29.1	24.3	19.9	0.7	10.4	11.5	9.5
LL	REINDL1	30	17.9	13.5	11.7	-11	-1.7	-0.3	-0.4
	ERBS	30.2	16.8	13.2	11.9	-12.5	0.6	1.6	0.7
	REINDL2	26.9	17.3	14.2	14.2	-2.4	-0.2	-4.8	-8
	MAXWELL	32.7	19.8	12.8	15.2	18.7	11	-1.1	-10
	LOPEZ	29	18.9	13.5	11.5	7	6.2	1.9	-0.9
	LOUCHE	27.8	18.3	14.7	13	-4.7	6.4	7.1	6.1
M	REINDL1	36	20.5	14.3	11.3	-19.4	-7.8	-2.3	-0.8
	ERBS	37.1	18.9	13.9	11.9	-21.6	-6.1	-0.8	-0.3
	REINDL2	31.1	19.5	16	14.5	-11.5	-6.9	-7.3	-8.8
	MAXWELL	28.3	17.7	15.4	18	6.7	1.9	-6.2	-13.6
	LOPEZ	29.8	19	14.2	11.3	-2	-0.1	0	-0.9
	LOUCHE	32.8	18.1	14.6	12.7	-13.9	-0.4	4.7	5.4
CC	REINDL1	33.9	18.8	14.9	11.8	-14.6	-4	0.5	0.6
	ERBS	33.9	17.6	15.1	12.5	-15.3	-2	1.2	0.2
	REINDL2	29.8	18.1	16.1	14.3	-6.9	-2.9	-5.1	-7.5
	MAXWELL	30.2	18.4	14.7	14.4	11.8	6.7	-1	-8.5
	LOPEZ	30.9	19	15.4	11.9	1.6	3.5	3.1	1.1
	LOUCHE	31.2	18.1	16.4	13.5	-8.3	3.5	7	6.2
MU	REINDL1	33.5	18.8	15.8	14.1	-12.2	-2.2	4.1	5.9
	ERBS	34.4	17.9	16.5	15.3	-15.2	-0.1	6.2	7.3
	REINDL2	30.3	18.1	15.3	13.1	-3.6	-1.1	-1	-2.4
	MAXWELL	35.3	20.4	15.3	13.4	17.9	10.2	3.2	-4.4
	LOPEZ	31.6	19.5	16.5	13.9	7	5.6	6.4	5.2
	LOUCHE	31.3	19.1	19.4	18.5	-6.5	5.8	12	13.1

Table B.III. *Values of RMSE and MBE (in percentage) obtained from the comparison between estimated and measured data of diffuse solar irradiance, D_h, on hourly basis for six models and nine locations by considering different solar altitude angle ranges.*

	α(°)	DIFUSSE D_h							
		RMSE (%)				MBE (%)			
		<20	20-40	40-60	>60	<20	20-40	40-60	>60
S	REINDL1	33	30.6	30.8	34.4	9.5	-0.6	-9.2	-13.8
	ERBS	34.2	29.6	30.9	35.4	11.9	-1.4	-9.8	-13.6
	REINDL2	31.3	29.1	29.8	32.7	2	0.1	1.4	3.1
	MAXWELL	35.8	33.2	27.9	28.3	-15.6	-14.7	-6.2	3.9
	LOPEZ	34.4	36.2	32	32.9	-10	-13.8	-13.2	-12.6
	LOUCHE	32.6	32.2	35.8	40.6	3.5	-10.6	-20.9	-25.7
0	REINDL1	37.4	33.7	31	33	11.9	3.6	-4.6	-5.2
	ERBS	38.6	32.8	31.4	34	14.2	2.8	-5	-4.7
	REINDL2	34.9	32.6	31	34.4	4.3	2.8	5.3	11
	MAXWELL	38.3	34.7	30.3	36	-12.6	-10.2	2.2	16.4
	LOPEZ	37.9	35.7	32.1	33.3	-8.1	-9.1	-7.9	-3.3
	LOUCHE	36.4	33.9	34.7	37.2	5.7	-6.6	-15.3	-15.9
LE	REINDL1	42.5	34.6	36	38.2	21.8	1.6	-5.9	-5
	ERBS	41.1	33.6	37.9	41.4	21	-0.3	-4.5	-1.7
	REINDL2	36	36.3	42	46.3	9.4	2.4	12.8	21.1

	MAXWELL	37	36.1	33.8	42.2	-13.7	-14.7	2.9	24.8
	LOPEZ	37.5	39	39.4	37.8	-2.8	-15.2	-15.5	-11.1
	LOUCHE	37.4	36.2	41.7	43.8	10.8	-12.8	-20.3	-20.1
VA	REINDL1	49.2	38.9	37.1	38.8	27.7	10.4	4.5	4.7
	ERBS	49.7	36.5	36.9	41.3	29.4	7.7	2.9	5.5
	REINDL2	42.6	38.4	42.4	50.8	17.1	8.9	18.8	31.1
	MAXWELL	38.6	36.3	38.9	57	-6.5	-7.3	14.1	41.8
	LOPEZ	41.2	37.8	37.1	38.2	4.1	-4.8	-2.1	2.7
	LOUCHE	44.4	36.3	38.2	41.3	19.3	-3.8	-12	-13.7
SA	REINDL1	45.3	39.9	38.7	40.6	20.2	4.5	0.7	2.3
	ERBS	45.7	39	39.6	43.3	21.4	2.6	0.4	4.3
	REINDL2	41.4	40.2	44.3	51.7	10.4	3.8	16.3	29.1
	MAXWELL	42.2	40.7	40.1	55.5	-10	-11	10.3	38
	LOPEZ	42.8	41.6	39.3	39.5	-2.9	-10.4	-6.4	-0.7
	LOUCHE	42.4	40.1	41.6	43.9	11.8	-8.6	-14.8	-15.2
LL	REINDL1	42	33.9	34.2	35.9	23.8	8.2	3.9	3.9
	ERBS	42.2	30.6	33	36.6	25.6	3.9	-0.8	0.4
	REINDL2	35.1	32.3	37.3	45.2	13.1	5.4	15.4	27.1
	MAXWELL	34.6	33.3	32	47.7	-13.1	-15.8	6	33.4
	LOPEZ	34.7	33.2	33.5	35.3	1.4	-6.7	-1.4	5.5
	LOUCHE	37.1	31.6	35.5	38.5	15.9	-7.1	-14.6	-16.3
M	REINDL1	50.8	40.2	34.1	32.5	34.2	20.1	9.6	6.2
	ERBS	52.6	36.8	33.1	34.3	37.2	16.5	5.9	4.8
	REINDL2	42.5	38.2	40.3	45	23.5	18.1	22.7	30.7
	MAXWELL	33.5	32.8	39.1	56.9	-1.2	0.2	19.9	45.5
	LOPEZ	37.9	35.4	33.3	32.6	10.6	4.4	3.7	6.6
	LOUCHE	45.2	33.7	33.4	35	26.8	4.9	-8.5	-12.7
CC	REINDL1	52.2	40	36.3	36.3	32.9	15.8	7.1	7
	ERBS	52	36.4	36.7	39.4	33.9	11.4	5.2	8.2
	REINDL2	43.6	38.7	44.2	51.2	21.1	13.5	22.8	34.8
	MAXWELL	36.5	35.1	36.7	51.5	-7.6	-8.4	11.3	38
	LOPEZ	41.2	37	35.6	35.5	8.1	-1.1	-0.4	5.3
	LOUCHE	45.5	34.9	37.1	38.3	23.3	-1.2	-11.1	-12.2
MU	REINDL1	38.8	33.9	29	29.5	21.3	12	-0.8	-6.8
	ERBS	40	31	29.6	32.1	24.5	8.1	-5.2	-10.2
	REINDL2	33	32.2	31.1	32.4	12.1	10.1	10.3	14.4
	MAXWELL	31.9	31.3	28.5	34.2	-11.1	-10.9	1.2	19.4
	LOPEZ	31.6	31.6	29.5	29	0.6	-2.3	-5.7	-5.1
	LOUCHE	34.7	30.4	33.9	38.5	15.2	-2.8	-17.7	-24.8

REFERENCES

1 Communication from the European Parliament, the Council, the European Economic and Social Committee and the Committee of the Regions: Energy Roadmap 2050. (COM/2011/0885 final).

2 Stoffel, T., Renné, D., Myers, D., Wilcox, S., Sengupta, M., George, R., Turchi., C., 2010. Concentrating solar power. Best Practices Handbook for the Collection and Use of Solar Resource Data. Technical Report NREL/TP-550-47465.

3 El Ouderni, A.R., Maatallah, T., El Alimi, S., Ben Nassrallah, S., 2013 Experimental assessment of the solar energy potential in the gulf of Tunis, Tunisia. Renewable and Sustainable Energy Reviews 20, 155–168

4 Zawilska, E.M., Brooks, J., 2011. An assessment of the solar resource for Durban, South Africa. Renewable Energy 36, 3433-3438.

5 Copper, J.K., Sproul, A.B., 2012. Comparative study of mathematical models in estimating solar irradiance for Australia. Renewable Energy 43, 130-139.

6 Khahro, S.F., Tabbassum, K., Talpur, S., Alvi, M.B., Xiaozhong Liao, Lei Dong, 2015. Evaluation of solar energy resources by establishing empirical models for diffuse solar radiation on tilted surface and analysis for optimum tilt angle for a prospective location in southern region of Sindh, Pakistan. Electrical Power and Energy Systems 64, 1073–1080.

7 Pérez-Higueras, P.J., Rodrigo, P., Fernández, E.F., Almonacid, F. Hontoria. L., 2012. A simplified method for estimating direct normal solar irradiation from global horizontal irradiation useful for CPV applications. Renewable and Sustainable Energy Reviews 16, 5529-34.

8 Vick, B.D., Myers, D.R., Boyson, W. E., 2012. Using direct normal irradiance models and utility electrical loading to assess benefit of a concentrating solar power plant. Solar Energy 86, 3519–3530.

9 Badescu, V., Gueymard, C.A. , Cheval, S. Oprea, C. Baciu, M. , Dumitrescu, A., Iacobescu, F., Milos, I., Rada, C., 2013. Accuracy analysis for fifty-four clear-sky solar radiation models using routine hourly global irradiance measurements in Romania. Renewable Energy 55, 85-103.

10 Gueymard, C.A., Ruiz-Arias, J.A., 2016. Extensive worldwide validation and climate sensitivity analysis of direct irradiance predictions from 1-min global irradiance. Solar Energy 128, 1–30.

11 Gueymard, C.A., Wilcox, S.M., 2011. Assessment of spatial and temporal variability in the US solar resource from radiometric measurements and predictions from models using ground-based or satellite data. Solar Energy 85, 1068–1084.

12 Yao, W., Li, Z., Xiu, T., Lu, Y., Li, X., 2015. New decomposition models to estimate hourly global solar radiation from the daily value. Solar Energy 120, 87–99.

13 Bertrand, C., Vanderveken, G., Journee, M., 2015. Evaluation of decomposition models of various complexity to estimate the direct solar irradiance over Belgium. Renewable Energy 74, 618-626.

14 Boland, J., Huang, J., Ridley, B., 2013. Decomposing global solar radiation into its direct and diffuse components. Renewable and Sustainable Energy Reviews 28, 749–756.

15 Dervishi, S., Mahdavi, A., 2012. Computing diffuse fraction of global horizontal solar radiation: A model comparison. Solar Energy 86, 1796-802.

16 Li, H., Bu, X., Long, Z., Zhao, L., Ma., W.,2012. Calculating the diffuse solar radiation in regions without solar radiation measurements. Energy 44, 611-615

17 Torres, J.L., De Blas, M., García, A., de Francisco, A., 2010. Comparative study of various models in estimating hourly diffuse solar irradiance. Renewable Energy 35,1325-32.

18 Bortolini, M., Gamberi, M., Graziani, A., Manzini, R., Mora, C., 2013. Multi-location model for the estimation of the horizontal daily diffuse fraction of solar radiation in Europe, Energy Conversion and Management 67, 208-216.

19 Yousif, C., Oña Quecedo, G., Bilbao Santos, J., 2013. Comparison of solar radiation in Marsaxlokk, Malta and Valladolid, Spain. Renewable Energy 49, 203-206.

20 Yang, D., Dong, Z., Nobre, A., Khoo, Y.S., Irutitijaroen, P.J., Walsh, W.M., 2013. Evaluation of transposition and decomposition models for converting global solar irradiance from tilted surface to horizontal in tropical regions. Solar Energy 97, 369–387

21 Pérez-Burgos, A., Díez-Mediavilla, M., Alonso-Tristán, C., Rodríguez-Amigo, M.C., 2017. Analysis of solar direct irradiance models under clear-skies: Evaluation of the improvements for locally adapted models. Journal of Renewable and Sustainable Energy, 9(2) 023703.

22 Louche, A., Notton, G.,Poggi, P., Simonnot, G., 1991. Correlations for direct normal and global horizontal irradiation on a French Mediterranean site. Solar Energy 46, 261-266.

23 SLL Lighting Handbook, 2009. The Society of Light and Lighting publications (CIBSE).

24 *SkyCalc* Users Guide, 2014. *https://Energydesignresources.com*

25 Janjai, S., Pattarapanitchai, S., Prathumsit, J., Buntoung, S., Wattan, R., Masiri. I. , 2014. A method for mapping monthly average hourly diffuse illuminance from satellite data in Thailand, Solar Energy 102, 162–172.

26 Oteiza, P., Pérez-Burgos, A., 2012. Diffuse illuminance availability on horizontal and vertical surfaces at Madrid, Spain. Energy Conversion and Management 64, 313-319

27 Pérez-Burgos, A., Román, R., Bilbao, J., de Miguel, A., Oteiza, P., 2015. Reconstruction of long-term direct solar irradiance data series using a model based on the Cloud Modification Factor, Renewable Energy 77, 115–124

28 Choosri, P., Janjai, S., Nunez, M., Buntoung, S., Chanalert W., 2017. Development of a method for mapping monthly average hourly diffuse erythemal ultraviolet radiation, Journal of Atmospheric and Solar-Terrestrial Physics 161, 19–27.

29 Li, D.H., Lam, J.C., Lau, C.C.S., 2002. A new approach for predicting vertical global solar irradiance. Renewable energy 25, 591-606.

30 Maxwell, A.L. , 1987. A quasi-physical model for converting hourly global horizontal to direct normal insolation. Report SERI/TR-215-3087, Solar Energy Research Institute. Golden, CO. USA.

31 Reindl, D.T., Beckman, W.A., Duffie, J.A., 1990. Diffuse fraction correlations. Solar Energy 45, 1-7.

32 Erbs, D.G., Klein, S.A., Duffie, J.A., 1982. Estimation of the diffuse radiation fraction for hourly, daily and monthly-average global radiation. Solar Energy 28, 293-302.

33 López, G., Rubio, M.A., Batlles, F.J., 2000. Estimation of hourly direct normal from measured global solar irradiance in Spain. Renewable Energy 21,175-86.

34 López, G. and Gueymard, C. A., 2007. Clear-sky solar luminous efficacy determination using artificial neural networks. Solar Energy 81, 929–939.

35 Bachour, D., Perez-Astudillo, D., 2014. Ground measurements of Global Horizontal Irradiation in Doha, Qatar. Renewable Energy 71, 32-36.

36 El Chaar, L., Lamont, L.A., 2010. Global solar radiation: Multiple on-site assessments in Abu Dhabi, UAE. Renewable Energy 35, 1596–1601

37 Jamil, B. and Akhtar, N.,2017. Empirical models for estimation of diffuse solar radiation based on measured data for humid-subtropical climatic region of India. Journal of Renewable and Sustainable Energy 9, 033702.

38 Kambezidis, H.D., Kaskaoutis, D.G., Kharol, S. K., Moorthy, K.K., Satheesh, S.K., Kalapureddy, M.C.R., Badarinath, K.V.S., Sharma, A. R., Wild, M., 2012. Multi-decadal variation of the net downward shortwave radiation over south Asia: The solar dimming effect. Atmospheric Environment 50, 360-372.

39 Evseev, E.G. , Kudish, A.I., 2015. Analysis of solar irradiation measurements at Beer Sheva, Israel from 1985 through 2013. Energy Conversion and Management 97, 307-314.

40 Pérez-Burgos, A., Bilbao, J., De Miguel, A., Roman, R., 2014. Analysis of solar direct irradiance in Spain. Energy Procedia 57, 1010-1076

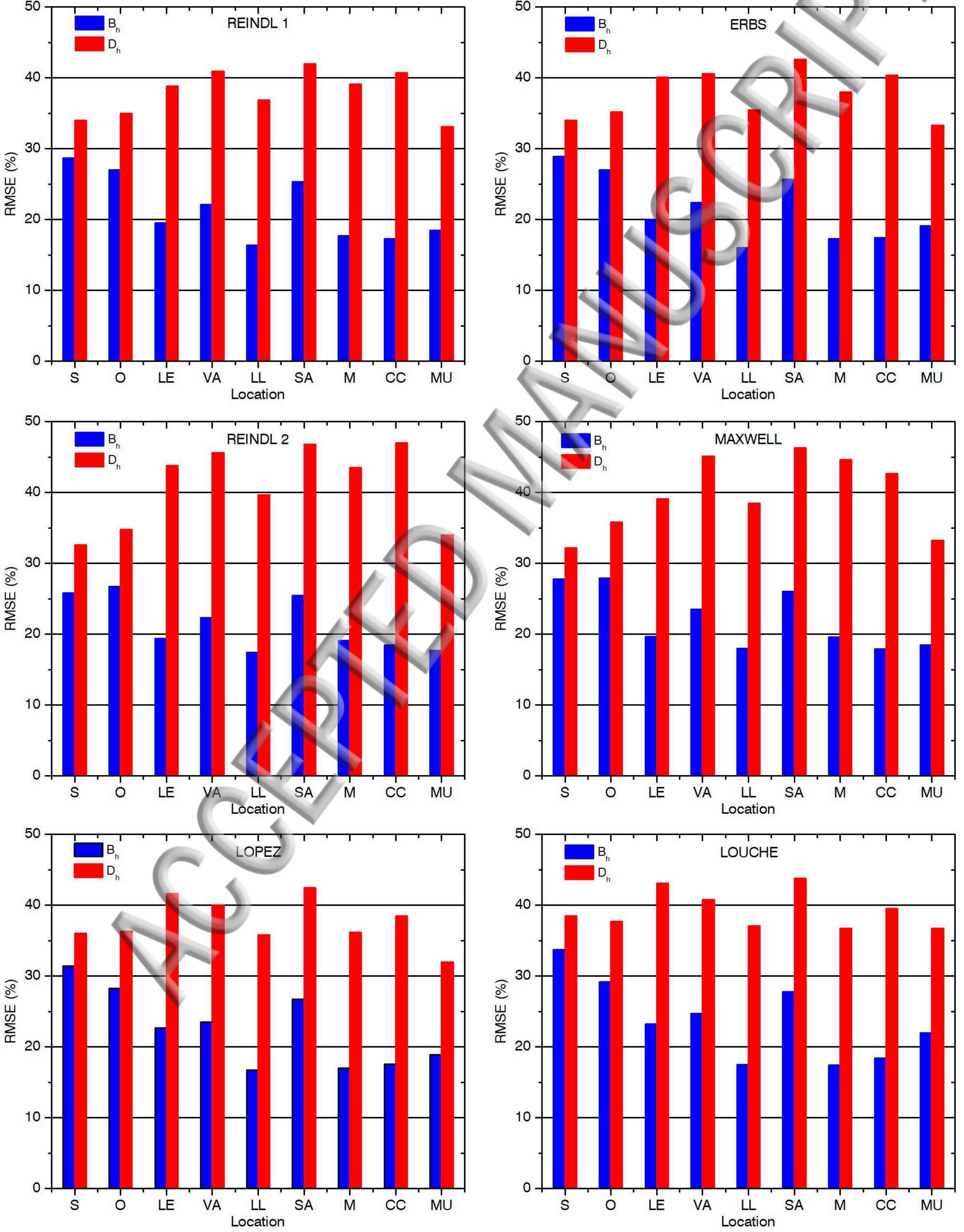
REINDL 1
ERBS
REINDL 2
MAXWELL
LOPEZ
LOUCHE
B_h
D_h
RMSE (%)
Location
S
O
LE
VA
LL
SA
M
CC
MU
0
10
20
30
40
50

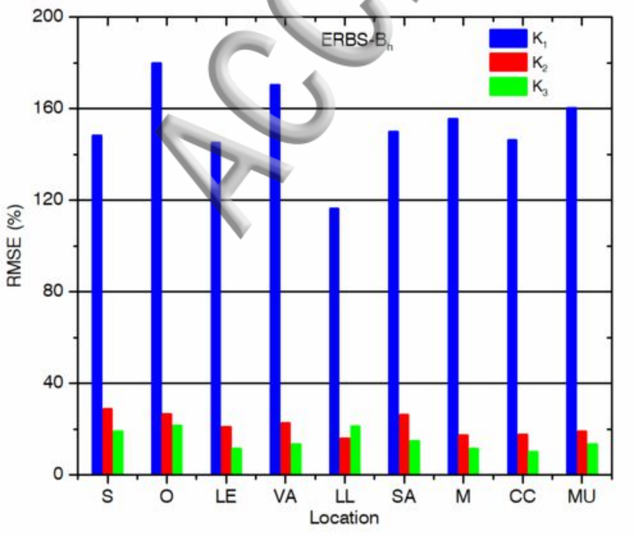

ERBS-B_h
K_1
K_2
K_3
200
160
120
80
40
0
RMSE (%)
S
O
LE
VA
LL
SA
M
CC
MU
Location

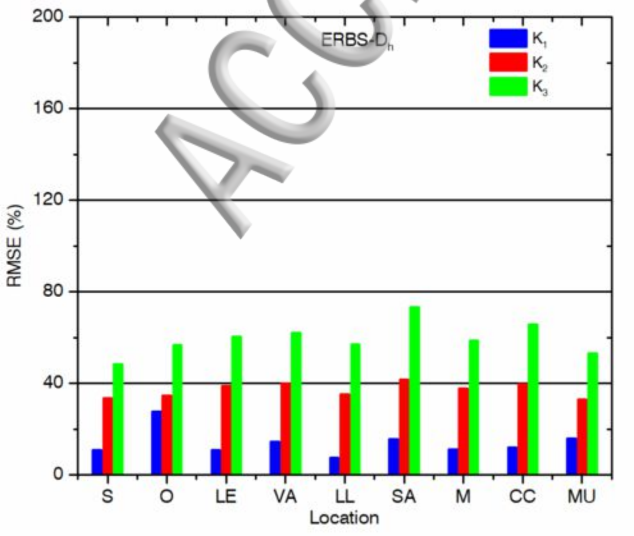

ERBS-D_h
K_1
K_2
K_3
RMSE (%)
200
160
120
80
40
0
S
O
LE
VA
LL
SA
M
CC
MU
Location

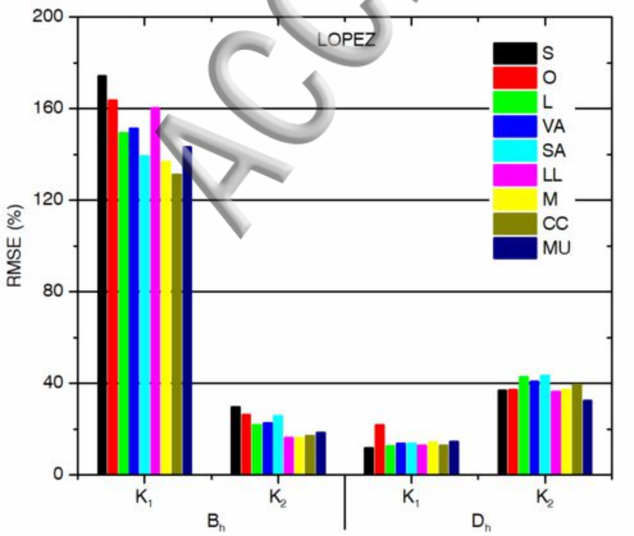

LOPEZ
S
O
L
VA
SA
LL
M
CC
MU
RMSE (%)
200
160
120
80
40
0
K_1
K_2
K_1
K_2
B_h
D_h

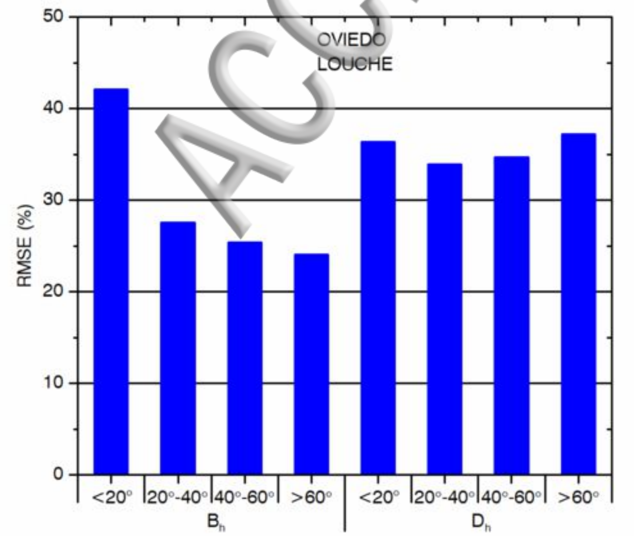

50
40
30
20
10
0
RMSE (%)
OVIEDO
LOUCHE
<20°
20°-40°
40°-60°
>60°
<20°
20°-40°
40°-60°
>60°
B_h
D_h

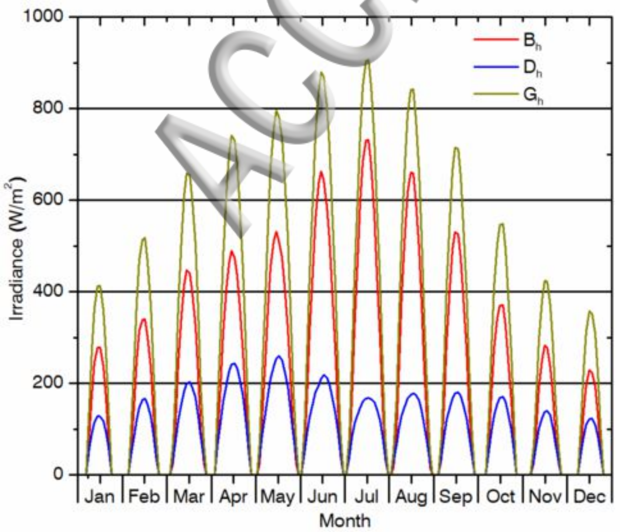

1000
800
600
400
200
0
Irradiance (W/m^2)
B_h
D_h
G_h
Jan
Feb
Mar
Apr
May
Jun
Jul
Aug
Sep
Oct
Nov
Dec
Month

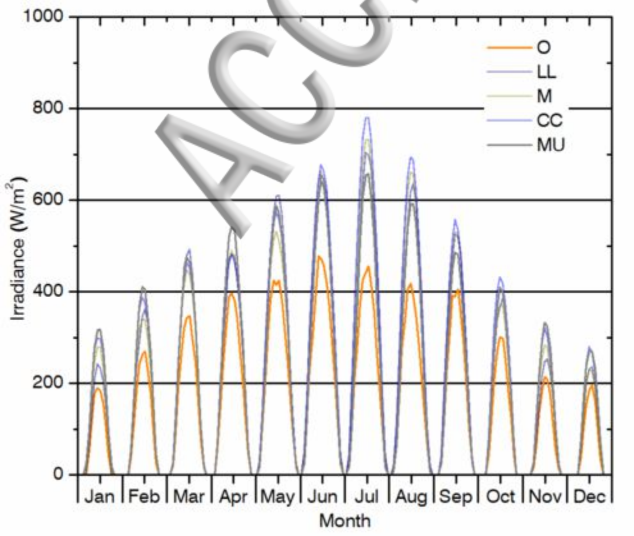

1000
800
600
400
200
0
Irradiance (W/m²)
O
LL
M
CC
MU
Jan
Feb
Mar
Apr
May
Jun
Jul
Aug
Sep
Oct
Nov
Dec
Month

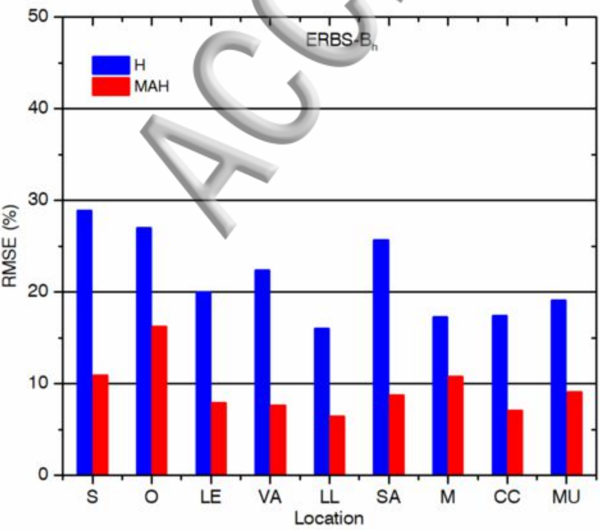
ERBS-B_h
H
MAH
RMSE (%)
0
10
20
30
40
50
S
O
LE
VA
LL
SA
M
CC
MU
Location

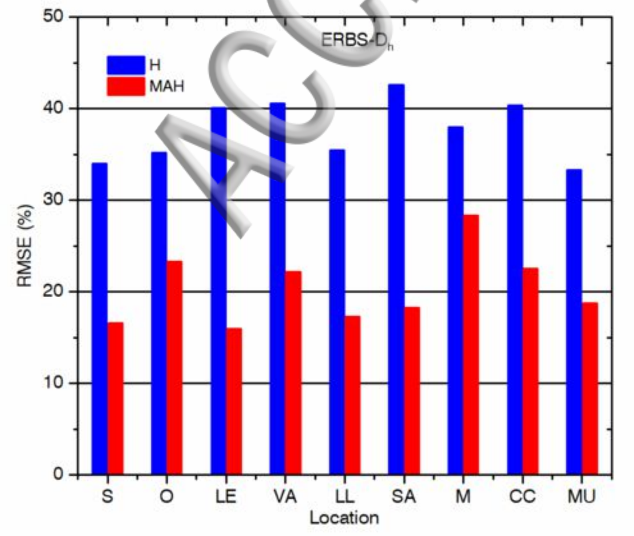
ERBS-D_h
H
MAH
RMSE (%)
0
10
20
30
40
50
S
O
LE
VA
LL
SA
M
CC
MU
Location

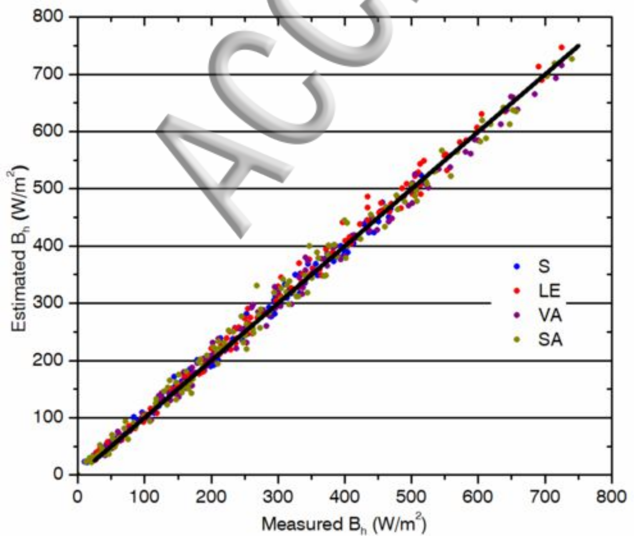

ACC
800
700
600
500
400
300
200
100
0
Estimated B_h (W/m^2)
S
LE
VA
SA
0
100
200
300
400
500
600
700
800
Measured B_h (W/m^2)

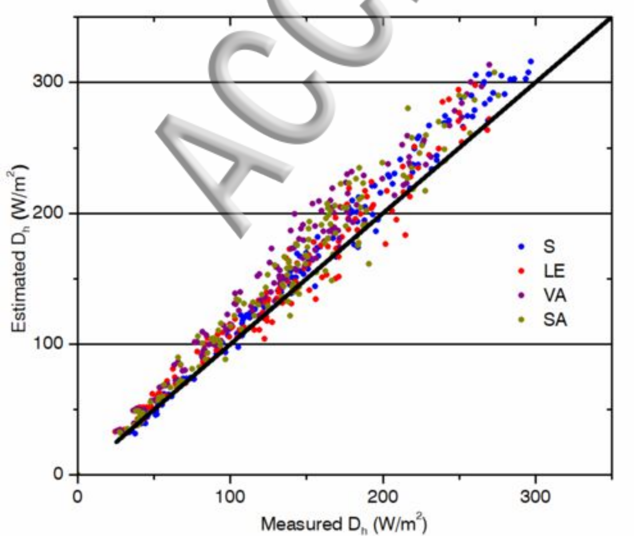

300
200
100
0
Estimated D_h (W/m^2)
0
100
200
300
Measured D_h (W/m^2)
S
LE
VA
SA

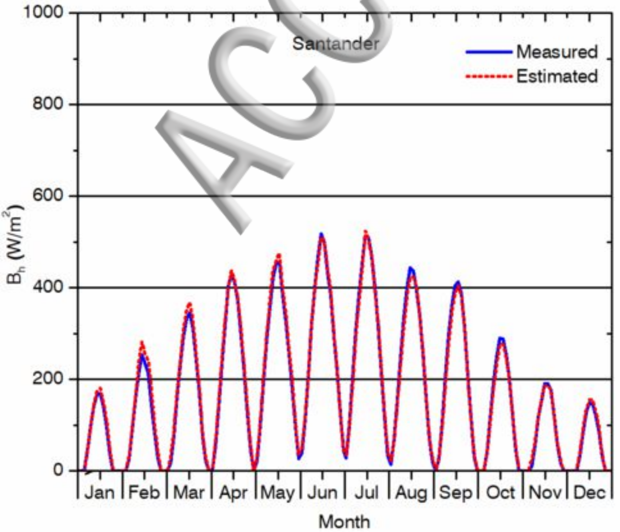

1000
800
600
400
200
0
Santander
Measured
Estimated
B_h (W/m^2)
Jan
Feb
Mar
Apr
May
Jun
Jul
Aug
Sep
Oct
Nov
Dec
Month

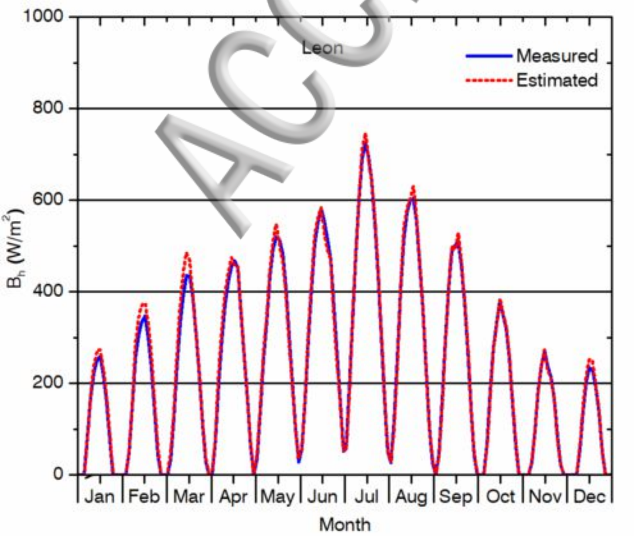

Leon
Measured
Estimated
B_h (W/m^2)
1000
800
600
400
200
0
Jan
Feb
Mar
Apr
May
Jun
Jul
Aug
Sep
Oct
Nov
Dec
Month

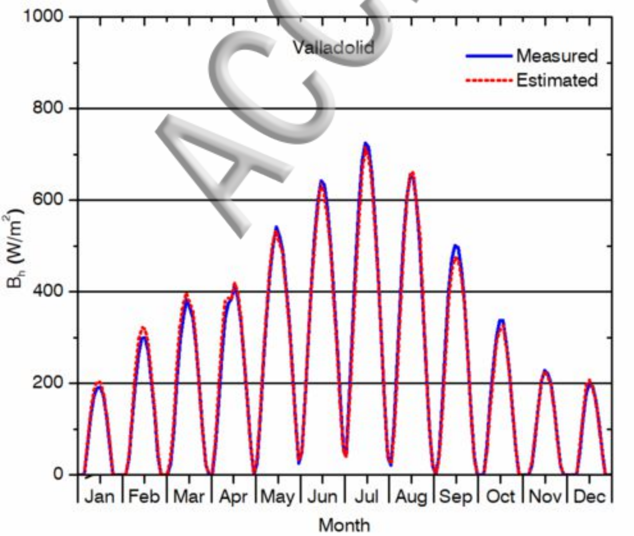

Valladolid
Measured
Estimated
B_h (W/m^2)
1000
800
600
400
200
0
Jan
Feb
Mar
Apr
May
Jun
Jul
Aug
Sep
Oct
Nov
Dec
Month

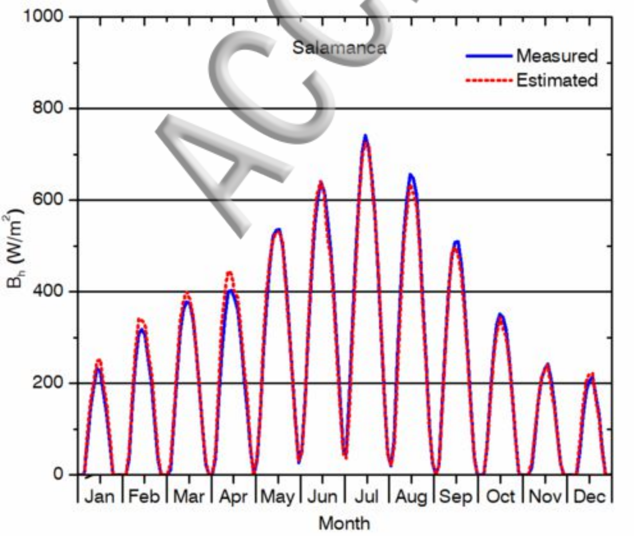
Salamanca
Measured
Estimated
1000
800
600
400
200
0
B_h (W/m^2)
Jan
Feb
Mar
Apr
May
Jun
Jul
Aug
Sep
Oct
Nov
Dec
Month

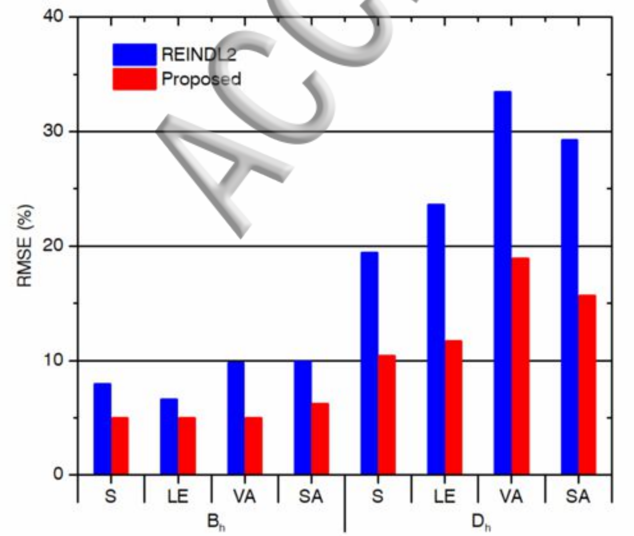
REINDL2
Proposed
RMSE (%)
0
10
20
30
40
S
LE
VA
SA
S
LE
VA
SA
B_h
D_h